

Published in final edited form as:

Circ Cardiovasc Imaging. 2015 January 30; 8(1): . doi:10.1161/CIRCIMAGING.114.001998.

Extracellular Volume Fraction Is More Closely Associated With Altered Regional Left Ventricular Velocities Than Left Ventricular Ejection Fraction in Non-Ischemic Cardiomyopathy

Jeremy Collins, MD¹, Cort Sommerville, MD¹, Patrick Magrath, MS², Bruce Spottiswoode, PhD³, Benjamin H Freed, MD⁴, Keith H Benzuly, MD⁴, Robert Gordon, MD⁴, Himabindu Vidula, MD⁴, Dan C Lee, MD⁴, Clyde Yancy, MD⁴, James Carr, MD¹, and Michael Markl, PhD^{1,2}

¹Department of Radiology, Feinberg School of Medicine, Northwestern University, Chicago, IL

²Department of Biomedical Engineering, McCormick School of Engineering, Northwestern University, Chicago, IL

³Siemens Medical Solutions USA, Chicago, IL

⁴Division of Cardiology, Department of Medicine, Feinberg School of Medicine, Northwestern University, Chicago, IL

Abstract

Background—Non-ischemic cardiomyopathy (NICM) is a common cause of left ventricular (LV) dysfunction and myocardial fibrosis. The purpose of this study was to non-invasively evaluate changes in segmental LV extracellular volume fraction (ECV), LV velocities, myocardial scar, and wall motion in NICM patients.

Methods and Results—Cardiac MRI including pre- and post-contrast myocardial T1-mapping and velocity quantification (tissue phase mapping, TPM) of the LV (basal, mid-ventricular, apical short axis) was applied in 31 patients with NICM (50±18years). Analysis based on the 16-segment AHA model was employed to evaluate the segmental distribution of ECV, peak systolic and diastolic myocardial velocities, scar determined by late gadolinium enhancement (LGE), and wall motion abnormalities. LV segments with scar or impaired wall motion were significantly associated with elevated ECV ($r=0.26$, $p<0.001$) and reduced peak systolic radial velocities ($r=-0.43$, $p<0.001$). Regional myocardial velocities and ECV were similar for patients with reduced ($n=12$, $ECV=0.28\pm0.06$) and preserved LV ejection fraction (LVEF) ($n=19$, $ECV=0.30\pm0.09$). Patients with preserved LVEF showed significant relationships between increasing ECV and reduced systolic ($r=-0.19$, $r=-0.30$) and diastolic ($r=0.34$, $r=0.26$) radial and long-axis peak velocities ($p<0.001$). Even after excluding myocardial segments with LGE, significant relationships between ECV and segmental LV velocities were maintained indicating the potential

Correspondence to Michael Markl, Ph.D. Department of Radiology Northwestern University 737 N. Michigan Avenue Suite 1600 Chicago, Illinois 60611 Phone: +1 312-695-1799 Fax: +1 312 926-5991 michael.markl@northwestern.edu.

Disclosures
None.

of elevated ECV to identify regional diffuse fibrosis not visible by LGE which was associated with impaired regional LV function

Conclusions—Regionally elevated ECV negatively impacted myocardial velocities. The association of elevated regional ECV with reduced myocardial velocities independent of LVEF suggests a structure-function relationship between altered ECV and segmental myocardial function in NICM.

Keywords

non-ischemic cardiomyopathy; myocardial velocities; fibrosis; extracellular volume fraction; T1 mapping

The non-ischemic cardiomyopathies (NICM) comprise a diverse group of primary and secondary disorders of the myocardium¹. Although patient prognosis with a NICM is generally better than with an ischemic cardiomyopathy (ICM), treatment and the likelihood of response to therapy is dependent on the specific underlying cardiomyopathy. Current diagnostic tools rely on clinical evaluation combined with assessment of global left ventricular function by echocardiography. Cardiac MRI has evolved as a valuable tool in the diagnostic work-up of cardiomyopathies, combining quantitation of global cardiac function with regional myocardial scar evaluation²⁻⁵. Cardiac MRI has proven utility in the diagnosis of cardiac amyloidosis, hypertrophic cardiomyopathy (HCM), arrhythmogenic right ventricular cardiomyopathy (ARVC), and non-compaction cardiomyopathy, among others, and is able to differentiate these from ICM through the assessment of regional myocardial scar configuration.

However, myocardial scar assessment by delayed-enhancement imaging relies on contrast agent uptake in scar tissue relative to normal or “remote” myocardium. This approach is limited in patients with diffuse myocardial scar without discernable normal myocardium, a situation commonly encountered in myocardial amyloidosis. Moreover, the traditionally used measures of global LV systolic function may underestimate the impact of fibrosis on myocardial function and are insensitive to regional abnormalities in myocardial motion, particularly in patients with preserved left ventricular ejection fraction (LVEF).

Advances in cardiac MRI have enabled quantification of myocardial fibrosis through the calculation of the gadolinium extracellular volume fraction (ECV) using T1 mapping techniques employing the modified Look-Locker inversion recovery (MOLLI) method^{6,7}. Calculation of ECV can quantify both regional diffuse and patchy macroscopic myocardial scar and thus potentially improve the assessment of regional myocardial fibrosis⁸⁻¹⁰. In addition, tissue phase mapping (TPM), a technique employing a tri-directional phase contrast sequence mapped to the left ventricular short axes, can be used to quantify regional myocardial velocities over the cardiac cycle along all principal motion directions (radial, long-axis, circumferential) of the heart¹¹⁻¹⁵. TPM can thus be used to assess regional systolic and diastolic changes in myocardial velocities and may offer an improved sensitivity to detect regional functional abnormalities.

The aim of our study was to analyze in detail segmental ECV and regional myocardial velocities in NICM patients with preserved and with reduced LVEF and to test the hypothesis that NICM results in altered structure (increased ECV) and function (decreased systolic and diastolic myocardial peak velocities). In addition, we hypothesize that changes in regional ECV are more closely associated with impaired regional myocardial motion compared to global indices of LV systolic function such as the ejection fraction.

METHODS

Study Cohort

The study cohort was comprised of 31 symptomatic patients (15 men, age = 50±18 years) with NICM in normal sinus rhythm. Patients with primary or secondary causes of NICM were included; patients with a history of treated coronary artery disease without residual obstructive lesions in whom LV dysfunction was out of proportion to the extent of treated coronary artery disease were considered to have a NICM and were also included. Patient New York Heart Association (NYHA) stage of heart failure, American Heart Association heart failure stage, and current cardiac medications were obtained from the medical record. Where available within three months, transthoracic echocardiograms were reviewed to ascertain LV diastolic function. LVEF was defined as preserved at cardiac MR when >50%. All study subjects were included in accordance with an IRB protocol, which permitted retrospective chart review.

MR Imaging

MR imaging was performed on 1.5T systems (MAGNETOM Avanto, Aera, Siemens, Erlangen, Germany). All patients underwent standard cardiac MRI including late gadolinium enhancement (LGE) for the assessment of myocardial scar as well as ECG gated time-resolved (CINE) cardiac MRI for the evaluation of global cardiac function (LVEF, end diastolic volume (EDV), endsystolic volume (ESV), stroke volume (SV)) and LV mass. In addition, patients underwent both 2D tissue phase mapping (TPM) and T1 mapping in the short axis orientation at basal, midventricular, and apical levels.

T1-mapping was performed using a modified Look-Locker inversion recovery (MOLLI) technique as described previously by Messroghli and co-workers, utilizing a 17 heart beat acquisition comprising three Look-Locker cycles, separated by recovery periods of three heart beats⁷. The first and second Look-Locker cycles comprised three heartbeats and the third comprised five heartbeats. Data for each slice (base, mid, apex) were acquired during breath holding pre- and 10-25 minutes following the intravenous administration of a contrast agent bolus. Imaging reconstruction included motion correction of the MOLLI images with different inversion times, and the calculation of parametric LV T1 maps as described previously (Figure 1A)^{16, 17}. Imaging parameters were as follows: spatial resolution (pixel size)=2.3x1.8mm, slice thickness=8mm, flip angle=35°, acquisition time per short axis 2D slice=17 heart beats. Gadopentetate dimeglumine (Magnevist, Bayer Pharmaceuticals, Whippany, NJ) was administered as a bolus infusion at a dose of 0.2mmol/kg for eGFR >60 mL/min/1.73m² or at a dose of 0.1mmol/kg for eGFR 31-59mL/min/1.73m².

TPM consisted of a black-blood prepared CINE phase-contrast sequence with 3-directional velocity encoding (velocity sensitivity = 25cm/s)¹². Each short axis slice (basal, mid, and apical location) was acquired during a breath hold (Figure 1B). Data were acquired with temporal resolution=24ms; spatial resolution (pixel size)=2.9x2.4mm², slice thickness=8mm. Spatio-temporal imaging acceleration (k-t parallel imaging PEAK GRAPPA)¹⁸ with a net acceleration factor of $R_{net}=3.6$ was employed which permitted data acquisition during breath-holding (acquisition time per short axis 2D slice=25 heart beats).

Data Analysis - T1-Mapping

The hematocrit was collected within 48 hours of the MRI exam to calculate segmental extracellular volume fraction (ECV) as described by Jerosch-Harold and co-workers.⁵ By measuring the change in T1 within the blood pool and myocardium before after contrast agent administration and correcting for the hematocrit the ECV (volume of distribution of gadolinium contrast in the tissue) was calculated as:

$$ECV = (1 - hematocrit) \times \frac{\left(\frac{1}{T_1 \text{ myocardial post}} \right) - \left(\frac{1}{T_1 \text{ myocardial pre}} \right)}{\left(\frac{1}{T_1 \text{ blood post}} \right) - \left(\frac{1}{T_1 \text{ blood pre}} \right)} \quad (1)$$

Data Analysis - Tissue Phase Mapping

The TPM data were analyzed using in-house tools programmed in Matlab (The Mathworks, USA) for correcting background phase offsets, and extracting peak radial and longitudinal velocities at systole and diastole. Analysis included manual segmentation of the LV contours and transformation of the acquired tri-directional velocities into radial velocities representing contraction and expansion in the short axis and long-axis velocities as described previously^{19, 20}. Long-axis velocities were orthogonal to the short axis imaging plane. Velocities were defined as positive for systolic contraction / shortening. The resulting velocity components thus describe the myocardial velocities along the axes of the LV, i.e. radial contraction and expansion (radial velocities) and long-axis shortening and lengthening (long axis velocities).

Data Analysis - Regional T1, Myocardial Velocities and 16 Segment Model

As summarized in Figure 1, both regional ECV and LV short- and long-axis velocities, were mapped onto the American Heart Association (AHA) 16 segment model of the left ventricle²¹. The anteroseptal right ventricular LV insertion point was marked manually and the LV was divided according to the 16-segment model into 6 basal, 6 midventricular, and 4 apical regions of uniform arc lengths.

Mean segmental ECV values were calculated by manually drawing endocardial and epicardial ventricular borders on pre- and post-contrast T1 parametric map acquisitions. In addition, global left ventricular ECV was calculated for each subject as the average ECV over all 16 segments. In accordance with the work of Kellman evaluating the mean and standard deviation of LV ECV in normal subjects, LV segments with $ECV < 0.25$ were considered normal, segments with ECV between 0.25 and 0.29 (two standard deviations

above normal) were rated borderline, and segments with ECV ≥ 0.30 were considered elevated¹⁶.

For TPM, myocardial radial and long-axis velocities were also mapped onto the AHA 16-segment model by averaging velocities for all voxels within each myocardial segment. For all 16 segments, peak systolic and diastolic radial and long-axis velocities were extracted. In addition, global left ventricular systolic and diastolic peak radial and long-axis velocities were calculated for each subject as the average over all 16 segments.

Data Analysis - LGE and Wall Motion Abnormalities

Standard-of-care clinical LGE and cardiac CINE MRI data (basal, mid-ventricular and apical short axis orientations in all $n=31$ patients) were independently qualitatively evaluated by an experienced blinded observer (JC) based on the AHA 16-segment model. LGE analysis include the assessment of presence of delayed enhancement (hyper-enhancement compared to remote myocardium) for each segment using a 5-point grading system: 0: no enhancement, 1: enhancement affects $<25\%$ (1), 26-50% (2), 51-75% (3), $>75\%$ (4) of the segment volume. Regional wall motion was classified according to the following scheme: Normal wall motion (0), mildly hypokinetic (1), moderately hypokinetic (2), severely hypokinetic (3), akinetic (4), or dyskinetic (5).

Statistical Analysis

All MRI data (ECV, myocardial velocities, LGE findings, wall motion abnormalities) were mapped on the AHA 16-segment model. To compare the regional distribution of myocardial velocities between patient groups (low LVEF, preserved LVEF, normal ECV, borderline ECV, elevated ECV), a Lilliefors test was used to determine parameter normality followed by one-way ANOVA (normal distribution) or Kruskal Wallis (non-normal distribution). If the overall test was significant ($p<0.05$) a multiple comparisons procedure was performed. For each segment appropriate post-hoc tests (for Gaussian distributions t-tests, Mann-Whitney tests otherwise) were used for paired comparisons of data between patient groups (low vs. preserved LVEF, normal vs. borderline ECV, borderline vs. elevated ECV, normal vs. elevated ECV). The level of significance was adjusted for multiple testing by Bonferroni correction.

To identify relationships between ECV and LV velocities with basic hemodynamic and global cardiac function parameters, and between segmental myocardial peak velocities, ECV, LGE findings, and wall motion abnormalities, Pearson's (continuous variables) or Spearman's (ordinal data) correlation coefficients r and r_s were calculated. For the analysis of associations between region measures of velocities and ECV, data from all segments were included in the analysis.

RESULTS

Patient Cohort

As summarized in Tables 1 and 2, the patient cohort comprised $n=31$ subjects with NICM, subdivided clinically and by MRI as $n=13$ subjects with restrictive cardiomyopathy, $n=10$

subjects with dilated cardiomyopathy, n=3 subjects with hypertrophic cardiomyopathy, n=3 subjects with inflammatory cardiomyopathy, and n=2 subjects with non-classified cardiomyopathy. Transthoracic echocardiographically determined LV diastolic function grade, NYHA heart failure stage, AHA heart failure stage, and cardiac medications are listed in Table 2. Catheter angiography, stress testing or clinical workup demonstrated no evidence of coronary artery disease in 27 of 31 patients (87%). The remaining 4 patients had a history of remote (>2 years prior) percutaneous coronary intervention without residual significant disease and presented with clinical and imaging findings of a non-ischemic cardiomyopathy causing their symptoms.

Relationships with Age, Hemodynamic Parameters, and Global Cardiac Function

Basic hemodynamic parameters, global LV function, myocardial velocities, and ECV are summarized in Table 1. Global systolic radial and long-axis velocities were moderately but significantly ($p<0.05$) associated with LVEF ($r=0.51$ and $r=0.36$) and inversely correlated to ESV ($r=-0.44$ and $r=-0.39$). In addition, there was a significant relationship between increased LV mass-to-volume ratio and higher diastolic long-axis velocities ($r=0.42$). Correlation analysis revealed further associations between systolic radial velocities and SV ($r=0.39$) and between diastolic long axis velocities and age ($r=0.39$). Of note, blood pressure and heart rate did not influence myocardial velocities. For n=30 patients for whom NYHA classification was available (Table 2), correlational analysis revealed a significant relationship between increased NYHA grade and reduced peak systolic long axis velocities ($r=-0.54$, $p=0.002$) and elevated ECV ($r=0.45$, $p=0.012$).

Myocardial Velocities, native T1, and ECV - Low versus Preserved LVEF

Results of a subgroup analysis in patients with low and preserved LVEF (Table 1) showed that heart rate and blood pressure were similar between groups. Interestingly, levels of global left ventricular pre-contrast myocardial T1 (native T1) as well as ECV were similar between patients with reduced and preserved LVEF (native T1 = 1004 ± 44 vs 1001 ± 57 ; ECV= 0.28 ± 0.06 vs. 0.30 ± 0.09 , respectively). There were no regional differences in ECV between the reduced and preserved LVEF groups were detected (Figure 2C). Global systolic radial velocities were reduced ($p=0.02$) for low LVEF but all other myocardial velocity components were similar between groups (Table 1). Regional systolic velocities (Figure 2A) showed significant differences in only 3 (1) of 16 segments for radial (long-axis) velocities between patients with low and preserved LVEF. The distribution of diastolic peak velocities (Figure 2B) was similar for patients with low and preserved LVEF except for 1 segment with altered diastolic peak radial velocity.

Myocardial Velocities - Influence of ECV

Table 3 summarizes the comparison of regional LV peak velocities in myocardial segments with normal extracellular volume fraction (ECV 0.25) compared to those with borderline ($0.25<ECV<0.3$) and elevated (>0.3) ECV. Segments with elevated ECV demonstrated significantly reduced myocardial velocities compared to regions with normal ECV for systolic radial motion as well as long-axis velocities. Differences in LV velocities by ECV subgroup were most pronounced for systolic long-axis motion: 6.4 ± 1.1 cm/s for low ECV, 4.2 ± 1.7 cm/s for borderline ECV, 3.9 ± 1.5 cm/s for elevated ECV ($p<0.01$). In addition, there

was a significant relationship between increased ECV and higher native myocardial T1 ($r=0.60$, $p<0.001$).

LGE and Wall Motion Abnormalities

A total number of 72 myocardial segments with scar as demonstrated by LGE were found in 20/31 (55%) of NICM patients while wall motion abnormalities were present in 17/31 (65%) of subjects. As expected, LGE was found more frequently in NICM patients with elevated ECV (82%) compared to patients with normal (57%) or borderline ECV (54%). As summarized in Table 4, there were highly significant relationships between impaired regional wall motion and reduced LV peak velocities, which was most evident for radial systolic velocities ($r=-0.43$, $p<0.001$). In addition, the presence and extent of LGE was significantly associated with regionally elevated ECV ($r_S=0.26$, $p<0.001$).

Correlation of Regional Left Ventricular Velocities and ECV

For patients with preserved LVEF, correlation analysis (Figure 3) revealed moderate but significant relationships of regional LV systolic and diastolic radial and long-axis peak velocities with regional ECV. Increased ECV was significantly ($p<0.001$) associated with reduced systolic and diastolic peak velocities in both the short- and long-axes, linking regional myocardial ECV with altered regional myocardial velocities. For NICM patients with reduced LVEF, significant relationships between segments with elevated ECV and regionally altered myocardial velocities were found only for systolic peak velocities (radial: $r=-0.3$, $p<0.001$; long axis: $r=-0.46$, $p<0.001$).

Noticeably, excluding the 72 segments with visible LGE from the analysis, significant associations between segmental myocardial velocities and ECV were still present for systolic peak velocities (radial: $r=-0.15$, $p=0.001$; long axis: $r=-0.38$, $p<0.001$) and diastolic long-axis peak velocities ($r=0.18$, $p<0.001$).

DISCUSSION

The classical phenotypic description of ventricular function in heart failure has been restricted to LVEF and/or LV dimension measurements. The arbitrary partitioning of heart failure according to empirically derived measures of LVEF has resulted in overtly heterogeneous patient cohorts, which have in turn complicated clinical trial design and confused clinical trial results. Better phenotypic characterizations are needed especially for the assessment of those without evidence of ischemic heart disease.

The findings of this study demonstrate the potential of the combined application of advanced cardiac MRI techniques, T1-mapping and TPM, to detect regional alterations in left ventricular ECV and myocardial velocities. The integration of both methods in one MRI exam allowed for the co-registered evaluation of both segmental structural and functional abnormalities. Regional fibrosis burden, as quantified by ECV, was associated with impaired myocardial velocities in patients with NICM. This relationship was maintained even in patients with preserved global LV systolic function.

Our results suggest that elevated regional myocardial ECV adversely impacts regional function, reducing peak systolic and diastolic myocardial velocities. Even after excluding myocardial segments with LGE, significant relationships between ECV and segmental LV velocities were maintained. These findings demonstrate the potential of elevated ECV to identify regional diffuse fibrosis not visible by LGE that may be associated with impaired regional LV function. Importantly, LVEF as a global measure of systolic function was less sensitive to changes in myocardial structure, as evaluated with ECV, and was unable to predict altered regional myocardial peak systolic and diastolic velocities. This poor discriminatory function of the LVEF measurement should lead to a re-evaluation of how best to evaluate LV performance in the setting of heart failure and may serve as an explanation for the marked clinical heterogeneity in heart failure cohorts, especially heart failure with preserved ejection fraction.

LGE MRI, part of the standard-of-care cardiac MRI exam, has been extensively employed for the phenotypical assessment of ischemic and nonischemic cardiomyopathies and has provided new insights into pathophysiologic substrates²². A recent meta-analysis demonstrated that LGE has excellent prognostic characteristics to potentially guide risk stratification and management in NICM patients⁴.

Other studies, however, have shown that diffuse fibrosis or changes in ECV are difficult to assess with MRI using LGE.^{23, 24} As a result, T1-mapping and regional ECV quantification are of high interest as diagnostic tools for NICM¹⁰. A previous study comparing ECV in patients with hypertrophic cardiomyopathy and NICM compared with controls demonstrated significantly elevated ECV ($p < 0.01$)²⁵. Similarly, Iles and co-workers showed that T1 mapping could identify changes in myocardial T1 in heart failure, which appeared to reflect the presence of diffuse fibrosis²⁶. A recently reported study with 126 patients by Ugander et al. showed that ECV could quantitatively characterize myocardial infarction, atypical diffuse fibrosis, and subtle myocardial abnormalities not clinically apparent on LGE images.²⁷ In agreement with these findings we found a modest, but significant correlation between qualitatively assessed regional LGE and ECV ($r = 0.26$).

A number of previous studies have also investigated the relationship between myocardial ECV and cardiac function. Findings from a study by Jerosh-Herlod and co-workers in patients with idiopathic dilated cardiomyopathy demonstrated that changes in ECV correlated with reduced resting myocardial blood flow ($r = -0.56$; $p = 0.019$) and ventricular dilation ($r = 0.61$; $p < 0.01$)⁵. Another recent study investigated diffuse myocardial fibrosis and its association with myocardial dysfunction in congenital heart disease demonstrating that ECV correlated with the LV enddiastolic volume index ($r = 0.60$; $p < 0.001$) and negatively with LVEF ($r = -0.53$; $p < 0.001$)²⁸. Similar to our findings, both studies indicate that changes in ECV may be a key contributor to contractile dysfunction.

However, previous studies relied on measures of global cardiac function such as LVEF or ventricular dilatation for the assessment of impaired cardiac function, which may limit their potential to detect regional abnormalities in cardiac function. To our knowledge, the direct combination of the assessment of regional ECV with MRI techniques for the quantification of segmental changes in cardiac function as used in our study has not been reported to date.

We speculate that due to the patchy distribution of fibrosis in NICM in the myocardium, the combination of structural and functional imaging including all myocardial segments may help to complement the limited information from global LV function parameters and LGE MRI.

Assessment of regional myocardial wall motion abnormalities is important and can suggest acute inflammation (inflammatory cardiomyopathy), inflammation and/or scar (myocardial sarcoidosis) in patients with NICM. In our cohort, quantification of regional myocardial velocities correlated modestly but significantly with qualitative assessment of regional myocardial motion abnormalities ($r=-0.43$). Similar to our findings with TPM, LVEF alone was an insensitive predictor of regionally altered myocardial motion, as 47% (9 of 19) patients demonstrated regional myocardial motion abnormalities with a LVEF > 50%. Assessing regional myocardial velocities is thus of interest as a more sensitive marker for myocardial abnormalities over measures of global systolic and diastolic function alone.

Limitations

Limitations of our study include a small cohort size and the absence of a comparison to an age-matched control cohort without cardiac disease. In addition, the moderate correlation between increased segmental ECV and reduced LV peak velocities limits the significance of our findings and further studies with a larger number of subjects are needed to provide a better understanding of the relationship between ECV and TPM parameters. The heterogeneity of the study population (different types of cardiomyopathies) underscores the feasibility nature of the current study and precludes conclusions regarding the diagnostic impact of this approach characterizing cardiac abnormalities in NICM patients. Moreover, sub-group analysis such as eccentric vs. concentric LV remodeling could not be performed as it would be hampered by the relatively small size of the sub-groups. Nevertheless, the observed differences in myocardial velocities between segments with differences in ECV and the significant correlation between ECV and systolic and diastolic myocardial velocities indicate the potential of MRI to better understand the relationship between tissue abnormalities and functional deficits in NICM patients.

A drawback of the MR imaging protocol used in this study is related to the lengthy breath hold duration for the TPM acquisitions. In our cohort, 11 of 31 patients had signs of dyspnea, which may have led to incomplete breath holding during the TPM acquisition. Nevertheless, all TPM data could successfully be analyzed and data quality was sufficient for epi- and endocardial contour segmentation and calculation of regional peak velocities. It should also be noted that we did not normalize LV velocities for heart rate. However, both heart rate and blood pressure did not influence myocardial velocities (non-significant correlation ranging from $r=0.07$ to $r=0.18$). Although assessable by TPM, circumferential velocities and their role in non-ischemic cardiomyopathy were not investigated in this study. Previous studies showed that the circumferential motion of the myocardium is highly complex and can include up to five changes in rotational direction during the cardiac cycle in basal segments²⁹. It was thus difficult to clearly define systolic and diastolic time points for the segmental evaluation of circumferential velocities. Nevertheless, rotational motion

may be valuable for detecting functional deterioration in several forms of NICM and future studies are needed to systematically investigate its diagnostic value.

Investigators have studied multiple T1 MOLLI strategies to shorten the overall acquisition, while maintaining accuracy for T1 estimation across a range of heart rates. We employed the original T1 MOLLI approach in our study, acquiring T1 maps over a window of 17 heartbeats. Although the use of shorter breath-held T1 MOLLI techniques including Shortened MOLLI (ShMOLLI) (9 heart beats)³⁰ and saturation recovery single shot acquisition (SASHA) (10 heart beats)³¹ is advantageous in patients with limited breath-holding capabilities, T1 MOLLI images in our cohort were uniformly diagnostic. Recently, optimized shorter pre- and post-contrast MOLLI protocols (11 heartbeats) have been proposed which can help to reduce breath hold durations in future studies³².

The selection of the ECV ranges (normal, borderline, elevated) used in our study was based on previous studies¹⁶ but did not account for possible variability of ECV with age. In our cohort, no correlation of ECV with age was found ($p=0.12$) but the cutoff at $ECV=0.25$ between normal and borderline ECV needs to be validated in larger studies with a normal control cohort and different age groups.

ECV values are also dependent on the type of contrast infusion. A bolus approach, such as the one we applied, is easier to use in the clinical setting, but requires that the post-contrast T1 experiment is performed between 10- and 25-minutes following contrast administration. To date, few studies have addressed the unique influence of the chosen contrast agent on ECV values. Our cohort uniformly received gadopentetate dimeglumine at a dose of 0.1-0.2 mmol/kg, mitigating these confounding effects.

Conclusion

Our results demonstrate an inverse relationship between regionally elevated ECV and myocardial velocities suggestive of a structure-function relationship at the segmental level where increasing degrees of myocardial scar burden adversely impact regional systolic and diastolic function. Global assessment of left ventricular systolic function using the LVEF was less sensitive to regional myocardial changes in NICM. Segmental ECV and TPM analysis may be useful to detect early changes in patients with cardiomyopathies with focal regional involvement, such as hypertrophic cardiomyopathy, myocardial sarcoidosis and inflammatory cardiomyopathies among others.

Supplementary Material

Refer to Web version on PubMed Central for supplementary material.

Acknowledgments

Sources of Funding

Support by the National Heart, Lung, And Blood Institute (NHLBI) of the National Institutes of Health, grant 1R01 HL117888

References

1. Richardson P, McKenna W, Bristow M, Maisch B, Mautner B, O'Connell J, Olsen E, Thiene G, Goodwin J, Gyarfas I, Martin I, Nordet P. Report of the 1995 world health organization/international society and federation of cardiology task force on the definition and classification of cardiomyopathies. *Circulation*. 1996; 93:841–842. [PubMed: 8598070]
2. De Smet K, Verdries D, Tanaka K, De Mey J, De Maeseneer M. Mri in the assessment of non ischemic myocardial diseases. *Eur J Radiol*. 2012; 81:1546–1548. [PubMed: 21392911]
3. Gottlieb I, Macedo R, Bluemke DA, Lima JA. Magnetic resonance imaging in the evaluation of non-ischemic cardiomyopathies: Current applications and future perspectives. *Heart Fail Rev*. 2006; 11:313–323. [PubMed: 17131077]
4. Kuruvilla S, Adenaw N, Katwal AB, Lipinski MJ, Kramer CM, Salerno M. Late gadolinium enhancement on cmr predicts adverse cardiovascular outcomes in non-ischemic cardiomyopathy: A systematic review and meta-analysis. *Circ Cardiovasc Imaging*. 2014; 7:250–8. [PubMed: 24363358]
5. Jerosch-Herold M, Sheridan DC, Kushner JD, Nauman D, Burgess D, Dutton D, Alharethi R, Li D, Hershberger RE. Cardiac magnetic resonance imaging of myocardial contrast uptake and blood flow in patients affected with idiopathic or familial dilated cardiomyopathy. *Am J Physiol Heart Circ Physiol*. 2008; 295:H1234–H1242. [PubMed: 18660445]
6. Messroghli DR, Plein S, Higgins DM, Walters K, Jones TR, Ridgway JP, Sivananthan MU. Human myocardium: Single-breath-hold mr t1 mapping with high spatial resolution--reproducibility study. *Radiology*. 2006; 238:1004–1012. [PubMed: 16424239]
7. Messroghli DR, Radjenovic A, Kozerke S, Higgins DM, Sivananthan MU, Ridgway JP. Modified look-locker inversion recovery (molli) for high-resolution t1 mapping of the heart. *Magn Reson Med*. 2004; 52:141–146. [PubMed: 15236377]
8. Lee JJ, Liu S, Nacif MS, Ugander M, Han J, Kawel N, Sibley CT, Kellman P, Arai AE, Bluemke DA. Myocardial t1 and extracellular volume fraction mapping at 3 tesla. *J Cardiovasc Magn Reson*. 2011; 13:75. [PubMed: 22123333]
9. Liu S, Han J, Nacif MS, Jones J, Kawel N, Kellman P, Sibley CT, Bluemke DA. Diffuse myocardial fibrosis evaluation using cardiac magnetic resonance t1 mapping: Sample size considerations for clinical trials. *J Cardiovasc Magn Reson*. 2012; 14:90. [PubMed: 23272704]
10. Flett AS, Hayward MP, Ashworth MT, Hansen MS, Taylor AM, Elliott PM, McGregor C, Moon JC. Equilibrium contrast cardiovascular magnetic resonance for the measurement of diffuse myocardial fibrosis: Preliminary validation in humans. *Circulation*. 2010; 122:138–144. [PubMed: 20585010]
11. Markl M, Schneider B, Hennig J. Fast phase contrast cardiac magnetic resonance imaging: Improved assessment and analysis of left ventricular wall motion. *J Magn Reson Imaging*. 2002; 15:642–653. [PubMed: 12112514]
12. Jung B, Foll D, Bottler P, Petersen S, Hennig J, Markl M. Detailed analysis of myocardial motion in volunteers and patients using high-temporal-resolution mr tissue phase mapping. *J Magn Reson Imaging*. 2006; 24:1033–1039. [PubMed: 16947325]
13. Petersen SE, Jung BA, Wiesmann F, Selvanayagam JB, Francis JM, Hennig J, Neubauer S, Robson MD. Myocardial tissue phase mapping with cine phase-contrast mr imaging: Regional wall motion analysis in healthy volunteers. *Radiology*. 2006; 238:816–826. [PubMed: 16424246]
14. Delfino JG, Johnson KR, Eisner RL, Eder S, Leon AR, Oshinski JN. Three-directional myocardial phase-contrast tissue velocity mr imaging with navigator-echo gating: In vivo and in vitro study. *Radiology*. 2008; 246:917–925. [PubMed: 18223122]
15. Foll D, Jung B, Schilli E, Staehle F, Geibel A, Hennig J, Bode C, Markl M. Magnetic resonance tissue phase mapping of myocardial motion: New insight in age and gender. *Circ Cardiovasc Imaging*. 2010; 3:54–64. [PubMed: 19996380]
16. Kellman P, Wilson JR, Xue H, Bandettini WP, Shanbhag SM, Druey KM, Ugander M, Arai AE. Extracellular volume fraction mapping in the myocardium, part 2: Initial clinical experience. *J Cardiovasc Magn Reson*. 2012; 14:64. [PubMed: 22967246]

17. Kellman P, Wilson JR, Xue H, Ugander M, Arai AE. Extracellular volume fraction mapping in the myocardium, part 1: Evaluation of an automated method. *J Cardiovasc Magn Reson*. 2012; 14:63. [PubMed: 22963517]
18. Jung B, Honal M, Ullmann P, Hennig J, Markl M. Highly k-t-space-accelerated phase-contrast mri. *Magn Reson Med*. 2008; 60:1169–1177. [PubMed: 18958854]
19. Foell D, Jung BA, Germann E, Staehle F, Bode C, Hennig J, Markl M. Segmental myocardial velocities in dilated cardiomyopathy with and without left bundle branch block. *J Magn Reson Imaging*. 2013; 37:119–126. [PubMed: 22987362]
20. Jung B, Markl M, Foll D, Hennig J. Investigating myocardial motion by mri using tissue phase mapping. *Eur J Cardiothorac Surg*. 2006; 29(Suppl 1):S150–157. [PubMed: 16563784]
21. Cerqueira MD, Weissman NJ, Dilsizian V, Jacobs AK, Kaul S, Laskey WK, Pennell DJ, Rumberger JA, Ryan T, Verani MS. Standardized myocardial segmentation and nomenclature for tomographic imaging of the heart: A statement for healthcare professionals from the cardiac imaging committee of the council on clinical cardiology of the american heart association. *Circulation*. 2002; 105:539–542. [PubMed: 11815441]
22. Karamitsos TD, Neubauer S. The prognostic value of late gadolinium enhancement cmr in nonischemic cardiomyopathies. *Curr Cardiol Rep*. 2013; 15:326. [PubMed: 23250662]
23. Mewton N, Liu CY, Croisille P, Bluemke D, Lima JA. Assessment of myocardial fibrosis with cardiovascular magnetic resonance. *J Am Coll Cardiol*. 2011; 57:891–903. [PubMed: 21329834]
24. Gai N, Turkbey EB, Nazarian S, van der Geest RJ, Liu CY, Lima JA, Bluemke DA. T1 mapping of the gadolinium-enhanced myocardium: Adjustment for factors affecting interpatient comparison. *Magn Reson Med*. 2011; 65:1407–1415. [PubMed: 21500267]
25. Puntmann VO, Voigt T, Chen Z, Mayr M, Karim R, Rhode K, Pastor A, Carr-White G, Razavi R, Schaeffter T, Nagel E. Native t1 mapping in differentiation of normal myocardium from diffuse disease in hypertrophic and dilated cardiomyopathy. *JACC Cardiovasc Imaging*. 2013; 6:475–484. [PubMed: 23498674]
26. Iles L, Pfluger H, Phrommintikul A, Cherayath J, Aksit P, Gupta SN, Kaye DM, Taylor AJ. Evaluation of diffuse myocardial fibrosis in heart failure with cardiac magnetic resonance contrast-enhanced t1 mapping. *J Am Coll Cardiol*. 2008; 52:1574–1580. [PubMed: 19007595]
27. Ugander M, Oki AJ, Hsu LY, Kellman P, Greiser A, Aletras AH, Sibley CT, Chen MY, Bandettini WP, Arai AE. Extracellular volume imaging by magnetic resonance imaging provides insights into overt and sub-clinical myocardial pathology. *Eur Heart J*. 2012; 33:1268–1278. [PubMed: 22279111]
28. Broberg CS, Chugh SS, Conklin C, Sahn DJ, Jerosch-Herold M. Quantification of diffuse myocardial fibrosis and its association with myocardial dysfunction in congenital heart disease. *Circ Cardiovasc Imaging*. 2010; 3:727–734. [PubMed: 20855860]
29. Foll D, Jung B, Staehle F, Schilli E, Bode C, Hennig J, Markl M. Visualization of multidirectional regional left ventricular dynamics by high-temporal-resolution tissue phase mapping. *J Magn Reson Imaging*. 2009; 29:1043–1052. [PubMed: 19388130]
30. Piechnik SK, Ferreira VM, Dall'Armellina E, Cochlin LE, Greiser A, Neubauer S, Robson MD. Shortened modified look-locker inversion recovery (shmolli) for clinical myocardial t1-mapping at 1.5 and 3 t within a 9 heartbeat breathhold. *J Cardiovasc Magn Reson*. 2010; 12:69. [PubMed: 21092095]
31. Chow K, Flewitt JA, Green JD, Pagano JJ, Friedrich MG, Thompson RB. Saturation recovery single-shot acquisition (sasha) for myocardial t mapping. *Magn Reson Med*. 2014; 71:2082–95. [PubMed: 23881866]
32. Kellman P, Hansen MS. T1-mapping in the heart: Accuracy and precision. *J Cardiovasc Magn Reson*. 2014; 16:2. [PubMed: 24387626]

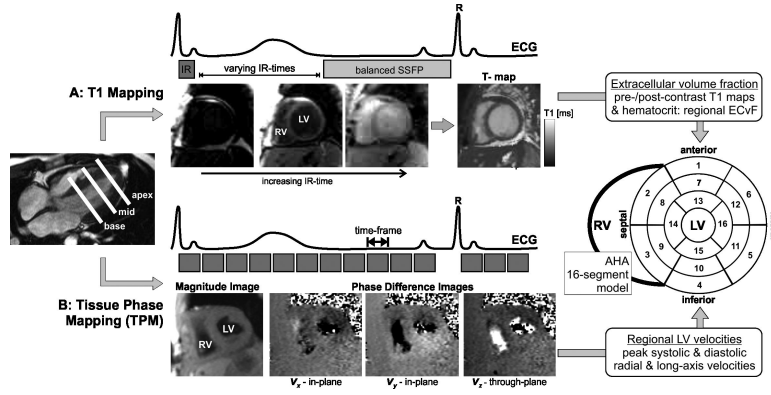


Figure 1. **A:** Combined T1 and Tissue Phase Mapping (TPM) for the comprehensive segmental evaluation of myocardial extracellular volume fraction (ECV) and function (3-directional left ventricular (LV) velocities). **A:** T1 mapping is based on diastolic balanced SSFP imaging with different inversion recovery (IR) times. **B:** Tissue phase mapping is based on ECG gated black-blood prepared phase contrast MRI with three-directional velocity encoding. Both T1 mapping and MVM were acquired in short axis orientation (base, mid, apex) during breath-holding. Results from both measurements were mapped on the AHA 16-segment model for direct segmental comparison of ECV and LV peak velocities.

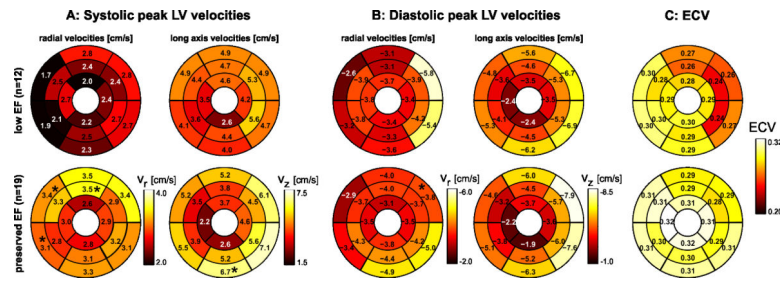


Figure 2.

A: Systolic left ventricular (LV) velocities in patients with non-ischemic heart disease with low EF (<50% (n=12) compared to a group of n=19 patients with preserved EF (>50%). The individual plots show the distribution of peak systolic radial and long-axis myocardial velocities in the AHA 16-segment model. **B:** Diastolic left ventricular (LV) velocities. **C:** LV mapping of extracellular volume fraction (ECV) derived from pre- and post-contrast T1-mapping in the same two patient groups. * Significant difference.

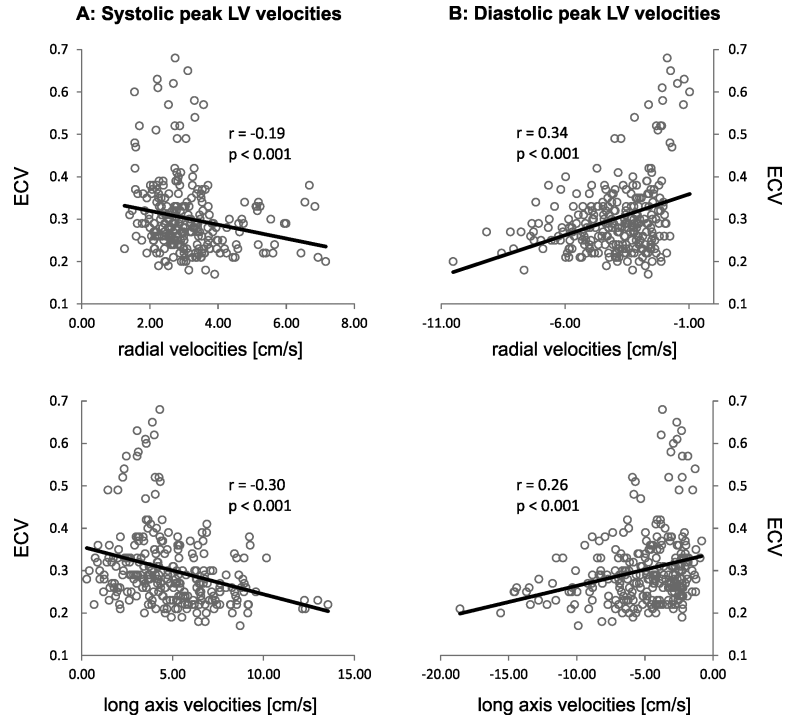


Figure 3. Correlation analysis between segmental systolic (A) and diastolic (B) LV peak velocities and regional myocardial extracellular volume fraction (ECV) in patients with nonischemic heart disease and preserved LVEF. The individual graphs show the results of the correlation of regional ECV with myocardial velocities for 19 patients with preserved LVEF on a segment-by-segment basis. For each subject, data from all 16 segments were included, resulting in a total of $19 \times 16 = 304$ data points (ECV - myocardial velocity pairs) for each graph.

Table 1

Descriptive statistics of patient demographics basic hemodynamic data, global cardiac function parameters and global myocardial velocities

	all patients	sub-group by LVEF		p-value
		low (<50%)	preserved (>50%)	
N	31	12	19	
age [years]	50±18 (54, 32)	45±18 (31, 21)	53±18 (59, 30)	0.20 *
LVEF [%]	49±17 (54, 21)	31±12* (31, 22)	60±5 (61, 9)	<0.001 *
EDV [ml]	170±68 (165, 69)	219±69* (199, 74)	138±47 (133, 52)	0.001 *
ESV [ml]	95±68 (68, 63)	156±73* (139, 97)	56±20 (53, 25)	<0.001 *
native T1 [ms]	1002±52 (995, 66)	1004±44 (994, 39)	1001±57 (995, 70)	0.86 *
SV [ml]	74±28 (72, 35)	60±21* (57, 16)	82±29 (80, 31)	0.032 *
LV mass [g]	128±50 (123, 63)	153±57* (145, 79)	113±40 (116, 58)	0.030 *
LV mass-to-volume ratio	0.79±0.22 (0.79, 0.35)	0.71±0.21 (0.71, 0.25)	0.84±0.21 (0.89, 0.29)	0.10 *
heart rate [bpm]	84±17 (82, 25)	89±21 (85, 31)	82±14 (80, 20)	0.28 *
systolic blood pressure [mmHg]	123±21 (120, 24)	125±22 (125, 41)	122±21 (116, 21)	0.66 *
diastolic blood pressure [mmHg]	78±14 (74, 20)	79±16 (77, 25)	77±12 (72, 18)	0.59 *
Number of LV segments with LGE	2.3±3.3 (1.0, 3.0)	1.3±1.6 (1.0, 2.3)	2.9±4.0 (2.0, 3.5)	0.31#
ECV [%]	0.29±0.08 (0.28, 0.02)	0.28±0.06 (0.27, 0.06)	0.30±0.09 (0.29, 0.06)	0.36#
radial vel. systole [cm/s]	2.9±1.0 (2.6, 0.6)	2.4±0.8* (2.5, 0.9)	3.2±1.0 (2.9, 0.4)	0.006#
radial vel. diastole [cm/s]	-3.9±1.0 (-3.6, 1.4)	-3.9±0.8 (-3.6, 1.3)	-4.0±1.1 (-3.6, 1.4)	0.80 *
long-ax vel. systole [cm/s]	4.6±1.8 (4.6, 2.9)	4.2±2.0 (3.6, 3.7)	4.8±1.6 (5.1, 2.6)	0.41 *
long-ax vel. diastole [cm/s]	-4.9±1.7 (-4.8, 1.9)	-4.9±1.1 (-4.8, 1.7)	-4.9±2.0 (-4.4, 2.5)	0.99 *

p-values: differences between sub-groups with low versus preserved LVEF for Gaussian distributions

Patient demographics, basic hemodynamic data, global cardiac function parameters and global myocardial velocities (averaged over all 16 segments of the LV) for the entire study cohort and for subgroups with low and preserved LVEF. Differences between sub-groups were evaluated using t-tests for Gaussian distributions (*). Otherwise, Mann-Whitney tests (#) were used. All data are presented as mean ± standard deviation (median, interquartile range).

* t-tests and non-normal distributions

Mann-Whitney tests

Table 2

Summary of cardiac medication use, NYHA heart failure status, AHA heart failure stage, and LV diastolic function assessment.

	N	Beta Blocker	Ca++ Channel Blocker	ACE-I ARB	Diuretic	Spirolactone	Digoxin
Cardiac Medication Classes	25	54.2% (13)	20.8% (5)	33.3% (8)	29.2% (7)	20.8% (5)	4.2% (1)
sub-group by LVEF							
low (<50%)	9	77.8% (7)	11.1% (1)	77.8% (7)	44.4% (4)	22.2% (2)	11.1% (1)
preserved (>50%)	16	37.5% (6)	25% (4)	6.3% (1)	18.8% (3)	18.8% (3)	0% (0)
		Normal	Grade I	Grade II	Grade III	Indeterminate	
Transthoracic Echocardiography	23	26.1% (6)	39.1% (9)	4.3% (1)	13% (3)	17.4% (4)	
		0	1	2	3	4	
NYHA Heart Failure Status	30	14% (4)	43% (13)	26% (8)	10% (3)	7% (2)	
		A	B	C	D		
AHA Heart Failure Stage	30	0% (0)	10% (3)	90% (27)	0% (0)		

Summary of cardiac medication use, NYHA heart failure status, AHA heart failure stage, and LV diastolic function assessment. N reflects the number of patients for who the respective information was available.

Table 3

Regional systolic and diastolic regional LV peak velocities

segments with	native T1 [ms]	ECV	radial vel. [cm/s]		long-ax vel. [cm/s]	
			systole	diastole	systole	diastole
normal ECV	968±23 (971, 33)	0.22±0.01 (0.22, 0.01)	3.3±0.8 (3.0, 1.0)	-3.6±0.4 (-3.5, 0.2)	6.4±1.1 (7.0, 1.4)	-4.9±0.8 (-4.9, 0.6)
borderline ECV	987±50 (992, 39)	0.27±0.01* (0.27, 0.02)	2.5±0.6* (2.5, 0.7)	-4.2±1.3 (-4.3, 1.2)	4.2±1.7* (3.4, 2.7)	-5.3±2.1 (-4.4, 3.0)
elevated ECV	1042±42 ^{+#} (1042, 71)	0.37±0.08 ^{+#} (0.35, 0.07)	3.0±1.3 (2.6, 0.4)	-3.8±1.2 (-3.3, 1.7)	3.9±1.5 [#] (3.4, 1.6)	-4.5±1.4 (-4.8, 2.6)

Regional systolic and diastolic regional LV peak velocities in myocardial segments with normal ECV±0.25, borderline ECV (0.25 ECV±0.3), and elevated ECV 0.3. All data are presented as mean ± standard deviation (median, interquartile range).

* significant difference normal ECV<0.25 versus borderline ECV=0.25-0.30

significant difference normal ECV<0.25 versus elevated ECV 0.30

⁺ significant difference borderline ECV=0.25-0.30 versus elevated ECV 0.30

Table 4

LGE and wall motion findings.

		radial vel. [cm/s]		long-ax vel. [cm/s]		ECV
		systole	diastole	systole	diastole	
LGE	r_s	-0.03	0.07	-0.07	<0.01	0.259*
	p-value	0.501	0.141	0.164	0.999	<0.001
wall motion	r	-0.43*	0.13*	-0.18*	0.03	-0.06
	p-value	<0.001	0.005	<0.001	0.566	0.224

Segment-by-segment comparison (AHA 16-segment model) of LGE and wall motion findings with ECV and LV peak velocities.